DOI: 10.1002/chem.200700958

# Fused Tricyclic Phosphiranes—Analysis of Phosphorus Chemical Shieldings

**Erik P. A. Couzijn,[a] Andreas W. Ehlers,[a] J. Chris Slootweg,[a] Marius Schakel,[a] Steffen Krill,[b] Martin Lutz,[c] Anthony L. Spek,[c] and Koop Lammertsma*[a, b]**

**Abstract:** 1,2-Addition of transient $W(CO)_5$-complexed phosphinidenes *exo* to hexamethyl Dewar benzene affords the novel 3-phosphatricyclo[3.2.0.0$^{2,4}$]hept-6-ene complexes. The fused tricyclic phosphiranes are obtained as both the *Z* and the thermally less stable *E* isomers, the $^{31}$P NMR chemical shifts of which differ by about 60 ppm. A computational investigation shows that the phosphorus pyramidalization and the presence of the γ double bond are responsible for this effect. The semiquantitative results contribute to a more systematic understanding of the structural influences on $^{31}$P chemical shieldings. The congested double bond of the *Z* isomer can be epoxidized with *m*-chloroperbenzoic acid (MCPBA) to afford a fused tetracyclic P,O bis-adduct.

**Keywords:** density functional calculations · fused-ring systems · NMR spectroscopy · phosphorus heterocycles · ring strain

## Introduction

Organophosphorus compounds constitute the largest ligand class for catalysis. Probing the ligand properties by $^{31}$P NMR spectroscopy would be highly desirable, but studies show only moderate or even counterintuitive relationships.[1,2] Phosphorus nuclear chemical shifts are governed by several factors, such as resonance interactions, inductive and steric effects, bond angles, and ring size.[2–4] Even the structurally very similar *Z* and *E* isomers of 7-phosphanorbornenes **1** differ by as much as 70 ppm in $^{31}$P NMR chemical shifts.[3] The advance of computing capacity allows for theoretical analyses of experimental systems.[2a,4,5] Chesnut et al.[4] related the variations in shielding to the magnitude of the HOMO–LUMO energy gap $E_g$ and addressed the underlying principles to qualitatively account for the variations, but noted that nonadditive α-, β-, and γ-substituent effects dominate the overall shielding.

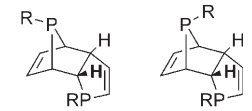


(*Z*)-**1a**: R = Ph
**b**: R = Me

(*E*)-**1a**,**b**

The 1,2-addition of carbene-like electrophilic phosphinidenes to alkenes gives direct access to both the *Z* and *E* isomeric phosphiranes,[6–9] providing suitable test systems for $^{31}$P NMR analysis. For example, the isomers of strained phosphiranes **2**[7] and **3**[8] show a difference in $^{31}$P chemical shielding analogous to **1**. Here, we report on phosphinidene addition to hexamethyl Dewar benzene (**9**) to give the novel

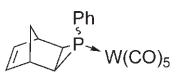


**2**

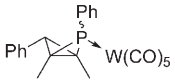


**3**

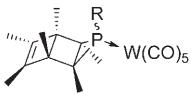


**4a**: R = Ph
**b**: R = Me

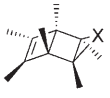


**5a**: X = $CH_2$
**b**: X = O
**c**: X = $S^+Ph$


**6a**: X = $CH_2$
**b**: X = O


**7**


**8**

[a] E. P. A. Couzijn, Dr. A. W. Ehlers, Dr. J. C. Slootweg, Dr. M. Schakel, Prof. Dr. K. Lammertsma
Department of Organic Chemistry
Faculty of Sciences, Vrije Universiteit
De Boelelaan 1083, 1081 HV, Amsterdam (The Netherlands)
Fax: (+31) 20-598-7488
E-mail: K.Lammertsma@few.vu.nl

[b] Dr. S. Krill, Prof. Dr. K. Lammertsma
Formerly associated with the Department of Chemistry
University of Alabama at Birmingham
Birmingham, AL 35294 (USA)

[c] Dr. M. Lutz, Prof. Dr. A. L. Spek
Crystal and Structural Chemistry
Bijvoet Center for Biomolecular Research
Utrecht University
Padualaan 8, 3584 CH Utrecht (The Netherlands)

Supporting information for this article is available on the WWW under http://www.chemeurj.org/ or from the author.

  

*exo*-annellated phosphiranes **4**, which have been characterized by NMR spectroscopy and X-ray crystallography. Also, the *Z* and *E* isomers of **4** have remarkably different $^{31}$P NMR chemical shifts. We explain the origins of this phenomenon semiquantitatively by a computational investigation, providing a more systematic understanding of structural influences on the $^{31}$P chemical shift.

Furthermore, adducts on hexamethyl Dewar benzene are scarce and, to the best of our knowledge, the phosphiranes **4** are the first isolated second-row element 1,2-adducts of **9**. First-row elements in mono- and bis-adducts of **9** are known, such as **5a**,**b** and **6**,[10,11] as are the nitrene adducts of hexafluoro Dewar benzene (**7** and **8**),[12] but only for **6b** has a crystal structure been reported.[11b] The intermediacy of the cationic sulfur analogue **5c** has been proposed, but it decomposes at −60 °C.[13] Therefore, we also report on the strain in **4** as well as on the reactivity of the remaining double bond in these fused tricyclic systems.

## Results and Discussion

**Synthesis**: Benzophosphepines **10** were recently developed,[14] from which transient terminal phosphinidene complexes [RP=W(CO)$_5$] were generated in situ under mild conditions (**10a**: R = phenyl, ≥55 °C; **b**: R = Me, ≥65 °C) by cheletropic elimination of naphthalene from the phosphanorcaradiene intermediate. Reaction of **10a**,**b** with **9** in toluene cleanly afforded the annellated phosphiranes **4a** and **4b** in 60 and 66% isolated yield, respectively (Scheme 1).[15]

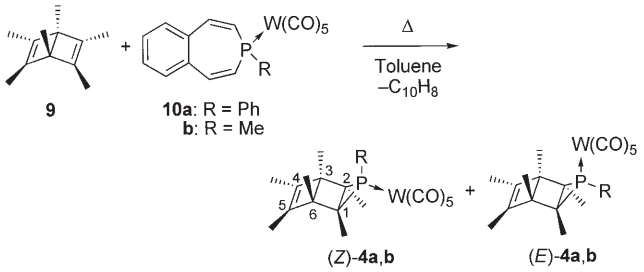


Scheme 1. Synthetic route to tricyclic phosphiranes **4**, including ring atom numbering.

Isomer (*Z*)-**4a** could be separated from the *E* isomer and purified by column chromatography and fractional crystallization to give a white crystalline solid that decomposes above 145 °C; **4b** could only be partially separated into isomerically enriched fractions.

NMR analysis of the products suggested that the phosphinidene complex has added *exo* to the double bond, while the phosphorus substituent R is oriented either *Z* or *E* with respect to the central cyclobutane moiety. For example, the 2D NOESY spectra for both isomers of **4a** feature an interaction of the phosphirane methyl (Me) groups (at C1/2) with those attached to the double bond, which would be absent in the *endo* adducts **11a**. Furthermore, correlations are observed for the phenyl *ortho*-H atoms with the central methyl groups (at C3/6) of the *Z* isomer and with the methyl groups of the phosphirane moiety (at C1/2) of the *E* isomer. The preference for the *exo* isomers is consistent with the addition of other heteroatom groups that lead to the *exo* adducts **5** and **6**,[10,11] and with the addition of [RP=W(CO)$_5$] to norbornene and related compounds.[16] This preference for *exo* addition has been attributed to rehybridization of the double bond(s) in the substrate, which causes a tilting of the p atomic orbitals of the carbon atom.[16b] As a result, the HOMO π electron density is more localized on the *exo* face than on the *endo* face, as illustrated for **9** in Figure 1.

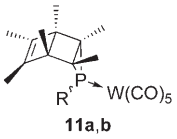


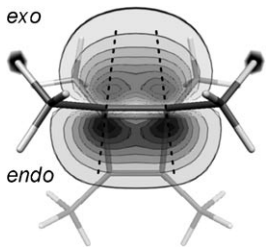


Figure 1. HOMO electron density distribution in **9**.

The $^{31}$P NMR chemical shifts of the products (**4a**: −63.0 (*Z*), −126.9 (*E*); **4b**: −87.3 (*Z*), −138.5 ppm (*E*)) are similar to those of the related norbornadiene adducts **2** (−61.0 (*Z*), −100.7 ppm (*E*)),[7] but are significantly deshielded relative to the parent phosphirane complexes **12a** (−187.6 ppm)[17] and **12b** (−199.3 ppm, see below).[18] The phosphirane carbon atoms resonate at rather low field (e.g. (*Z*)-**4a**: 49.3 vs. (*Z*)-**2**: 35.8 ppm).[7]

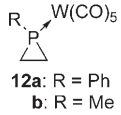


**Crystal structure**: The geometry of (*Z*)-**4a** was confirmed by X-ray crystallography (Figure 2). The crystal structure shows that the plane of the phenyl ring is parallel to the phosphirane C−C bond. This C1−C2 bond length of 1.592(4) Å is elongated in comparison to those in typical phosphiranes (1.47–1.52 Å)[7,17b,19] and is even longer than those in phosphabicyclobutane (*Z*)-**3** (1.550 Å).[8] The C3−C6 bridgehead bond is also elongated (1.588(4) Å), which is, however, common for cyclobutenes.[20] The central four-membered ring is planar and has interplanar angles of 118.57(19) and 110.22(19)° with the phosphirane and cyclobutene rings, respectively.[21] The central methyl groups (C9 and C12) are bent away from the phenyl group, as designated by the obtuse interplanar angle of 130.4(2)° with the central cyclobutane versus 119.3(2)° with the cyclobutene ring.[21]

**Calculated $^{31}$P NMR chemical shifts**: Because the $^{1}$H NMR resonances of the PMe group of **4b** and those of either its vinylic (*Z*) or phosphirane methyl groups (*E*) are in close proximity, the stereochemical assignment by 2D NOESY NMR is not unequivocal. Therefore, we calculated the phosphorus chemical shieldings $\sigma_{calcd}$ of the four possible adducts

  

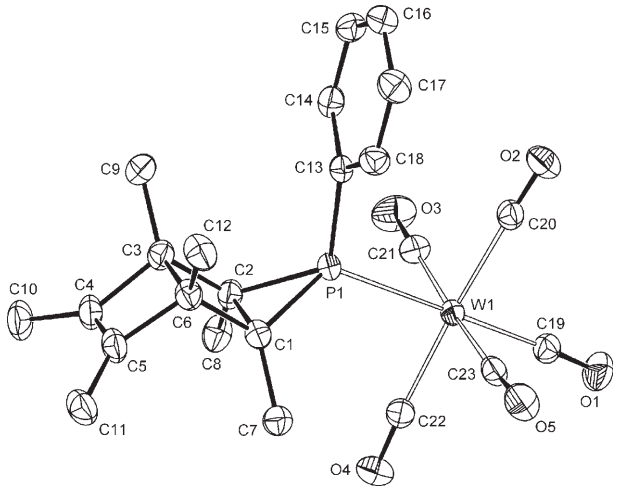


Figure 2. Displacement ellipsoid plot (50% probability) of (*Z*)-**4a**. Hydrogen atoms are omitted for clarity. Selected bond lengths (Å), angles and torsion angles (°): W1-P1 2.5206(7), P1−C1 1.831(3), P1−C2 1.840(3), C1−C2 1.592(4), C3−C6 1.588(4), C4−C5 1.334(4), C1-P1-C2 51.41(11), C2-C1-C7 127.1(2), C1-C2-C8 127.9(2), C3-C6-C12 125.6(2), C6-C3-C9 127.1(2), C5-C4-C10 135.1(3), C4-C5-C11 135.3(3), P1-C1-C2-C3 −118.68(16), P1-C2-C1-C6 118.46(16), C1-C6-C3-C4 110.15(19), C2-C3-C6-C5 −110.3(2), C1-C6-C3-C9 −130.7(3), C2-C3-C6-C12 130.2(3), C4-C3-C6-C12 −119.4(3), C5-C6-C3-C9 119.2(3).

(*exo*/*endo*, *Z*/*E*) with the Amsterdam Density Functional (ADF) program[22] at the BP86/TZP level of theory to confirm the stereochemistry of the products. The data in

Table 1. BP86/TZP $^{31}$P NMR chemical shieldings $\sigma$ and chemical shifts $\delta$ [ppm].

| | | $\sigma_{calcd}$ | $\delta_{calcd}$ | $\delta_{exptl}$ |
|---|---|---|---|---|
| **12b** | | 456.4 | −199.3[a] | −199.3 |
| **4a** | *Z* | 318.8 | −61.7 | −63.0 |
| | *E* | 387.1 | −130.0 | −126.9 |
| **4b** | *Z* | 338.9 | −81.8 | −87.3 |
| | *E* | 393.9 | −136.8 | −138.5 |
| **11b** | *Z* | 358.7 | −101.6 | |
| | *E* | 417.2 | −160.1 | |

[a] Used as reference chemical shift (see Experimental Section).

Table 1 show an excellent agreement between the computed and experimentally observed NMR chemical shifts of the *exo* adducts **4a**,**b** (e.g. (*Z*)-**4b**: $\delta = -81.8$ (exptl), −87.3 ppm (calcd); (*E*)-**4b**: $\delta = -138.5$ (exptl), −136.8 ppm (calcd)), while the *Z*- and *E*-*endo* adducts **11b** were predicted to be about 20 ppm more shielded as compared to **4b**.

**Phosphorus chemical shielding differences**: The *Z* isomers of **4a** and **4b** are as much as ≈60 ppm less shielded than the *E* isomers. Similar shielding differences between the *Z* and *E* isomers have been observed for the phosphinidene adducts **2**,[7] phosphabicyclobutanes **3**,[8] and 7-phosphanorbornenes **1**.[3] Next, we examined whether this difference has a sterical or electronic origin.

**Phosphorus chemical shielding analysis**: Chesnut et al. related the variations in shielding to the magnitude of the HOMO–LUMO energy gap $E_g$ and discussed the underlying principles.[4] They found that of the total shielding the diamagnetic term $\sigma_{Dia}$ varies little, as it relates to core terms that are similar for all phosphorus compounds, while the paramagnetic component $\sigma_{Para}$ varies much more. For uncomplexed phosphines, the HOMO represents the lone pair on the phosphorus, while the LUMO resembles an empty phosphorus p-orbital perpendicular to it. In an external magnetic field, effective coupling occurs between these molecular orbitals (MO),[23] and as the LUMO has a nodal plane through the phosphorus, this will cause a paramagnetic deshielding of the nucleus. A smaller energy gap $E_g$ leads to stronger MO coupling and, therefore, to a more negative $\sigma_{Para}$. The double bond in **1** has a large influence on the $^{31}$P chemical shielding by raising the HOMO, especially for the (*Z*)-**1** isomer that has its lone pair on the opposite side.[4a] In the tricyclic phosphiranes **4**, the double bond is more distant than in **1** (i.e., in the γ instead of the β position) and, therefore, we would expect a smaller effect.

The HOMO–LUMO gap is also influenced by the valence angles on phosphorus.[4d] Due to the steric requirements of the bridgehead methyl groups in **4** (relative to 1,3 diaxial steric interactions in cyclohexanes), the phosphorus atom is less pyramidal in the *Z* than in the *E* isomer according to our BP86/TZP calculations (i.e., the sum of the C-P-C angles: 279.2 (*Z*) and 254.7° (*E*)). To address this relationship for phosphiranes, we calculated the $^{31}$P NMR shieldings for uncomplexed phosphirane **12b′** (′ indicates no $W(CO)_5$), while varying the angle α between the P−Me bond and the phosphirane plane. The energy required for such deformations is modest, for example, +2.0 kcal mol$^{-1}$ for a 10° increase from the equilibrium value of 101.32° (see Figure 3a). Within the 20° range of α studied, the shielding changes more than 70 ppm (Figure 3a), which is fully attributable to $\sigma_{Para}$ and which is paralleled by a change in the HOMO–LUMO gap of 0.45 eV (Figure 3b, $E_g = 5.78$ at $\alpha = 95°$ and 5.34 eV at 115°). The p character of the P lone pair (HOMO) and, thus, its energy level, increases with larger angles α, resulting in decreasing pyramidalization, while the LUMO is much less affected. The same trend is observed for (*Z*)- and (*E*)-**3**, both of which have been characterized crystallographically. The phosphorus atom in (*Z*)-**3** is less pyramidal than that of the *E* isomer (the sum of the C-P-C angles: 273.9 vs. 259.9°, respectively), and, accordingly, is 48.4 ppm less shielded (*Z*: $\delta = -36.7$ ppm, *E*: $\delta = -85.1$ ppm).[8]

In complexes **4**, the metal fragment, which is both a σ acceptor and a π donor, lowers the energy of the P lone pair and raises that of the empty phosphorus p orbital.[5a] However, a more negative paramagnetic contribution is observed for **4b** than for uncomplexed **4b′**((*Z*)-**4b**: $\sigma_{Para} = -635.4$ ppm, (*Z*)-**4b′**: $\sigma_{Para} = -591.2$ ppm; see Table 2) which is due to extra deshielding contributions of the complex that arise from the coupling between the occupied π ($PR_3$) and virtual σ* (PW) orbitals.[5a] As these transitions complicate

  

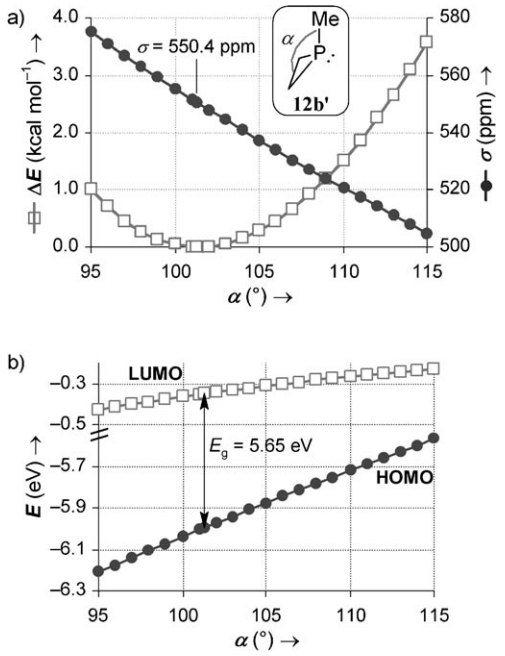


Figure 3. Effect of the phosphirane-Me angle α in **12b′** on a) the relative energy and the chemical shielding, and b) the HOMO and LUMO equilibrium gap energy $E_g$.

more detailed analyses, we focused on the uncomplexed model systems **4b′**, **13**, and **14** (Table 2). The paramagnetic contribution $\sigma_{Para}$ is much larger for the *E* than for the *Z* isomer of each model compound except for **14**; the differences in $\sigma_{Dia}$ are small. As the lone pair is more localized on P in **4b′** than in the complex **4b**, the phosphorus nucleus is more sensitive to the differences in the electronic structure of the isomers, which is expressed in an increase in $\Delta\sigma$ from 55 to 64 ppm.

To evaluate the influence of steric congestion on the P-pyramidalization, we replaced the bridgehead methyl groups in **4b′** with hydrogen atoms (**13**). The result is that the *Z* isomer becomes more pyramidal, as indicated by the angle $\alpha$ of 110.2° for (*Z*)-**13** versus 114.5° for (*Z*)-**4b′**. Consequently, the HOMO is lowered with a concomitant increase in $E_g$ from 4.33 to 4.44 eV. This effect is paralleled by a strong reduction of the paramagnetic deshielding from −591.2 for (*Z*)-**4b′** to −551.8 ppm for (*Z*)-**13**. In contrast, the *E* isomers show little structural change, and, hence, the $\sigma_{Para}$ contribution remains almost constant. Consequently, the difference in the total shielding $\sigma$ of the isomers is reduced from 64 for (*Z*/*E*)-**4b′** to 26 ppm for (*Z*/*E*)-**13** (Table 2).

The effect of the cyclobutene moiety becomes apparent when we compare model systems **13** and **14**, in which the unsaturated ring has been eliminated. The P-pyramidalization in the isomers of **13** and **14** is virtually unaffected (e.g., (*Z*)-**13**: $\alpha$ = 110.2°, (*Z*)-**14**: 110.0°), yet the influence on the chemical shift difference between the *E* and *Z* isomers is large. While this difference is substantial for **13** ($\Delta\sigma$ = 26.3 ppm), it vanished for **14** ($\Delta\sigma$ = −1.9 ppm). For (*Z*)-**14**, the $E_g$ is even larger than for its *E* isomer (5.30 vs. 5.02 eV, respectively), and the $\sigma_{Para}$ differs accordingly (−513.5 vs. −526.1 ppm), which thereby effectively counteracts the change in $\sigma_{Dia}$. The influence of the double bond becomes evident from the MO correlation diagrams for **13** and **14** that are shown in Figure 4. Compared to **14**, the π and π* components of the double bond in **13** participate in the HOMO and LUMO, respectively, causing a decrease in the energy difference $E_g$. Due to its relative orientation, the HOMO of the *Z* isomer is more destabilized (**14**: $E_{HOMO}$ = −5.50, **13**: −5.11 eV) than that of the *E* isomer (**14**: $E_{HOMO}$ = −5.27, **13**: −5.22 eV), resulting in a smaller HOMO–LUMO gap and, hence, a more negative $\sigma_{Para}$ ((*Z*)-**13**: −551.8, *E*: −534.0 ppm).

The fused phosphiranes **14** are much less shielded than the parent phosphirane **12b′** (compared to (*Z*)-**14**: $\sigma$ = 467.8, **12b′**: 550.4 ppm, see Figure 3) as a result of their higher

Table 2. $^{31}$P chemical shielding decompositions [ppm], phosphirane-Me angles $\alpha$ [°], and MO and gap energies [eV]; *Z* isomers drawn.

| | | | $\sigma_{Dia}$ | $\sigma_{Para}$ | $\sigma$ | $\alpha$ | $E_{HOMO}$ | $E_{LUMO}$ | $E_g$ |
|---|---|---|---|---|---|---|---|---|---|
| **4b** | 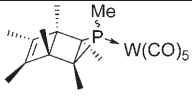 | *Z* | 974.3 | −635.4 | 338.9 | 117.4 | | | |
| | | *E* | 973.7 | −579.7 | 393.9 | 104.0 | | | |
| | | Δ | | | 55.1 | −13.4 | | | |
| **4b′** | 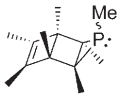 | *Z* | 983.1 | −591.2 | 391.9 | 114.5 | −4.95 | −0.62 | 4.33 |
| | | *E* | 987.8 | −531.8 | 456.0 | 103.3 | −5.11 | −0.51 | 4.60 |
| | | Δ | | | 64.1 | −11.2 | | | |
| **13** | 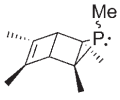 | *Z* | 980.1 | −551.8 | 428.2 | 110.2 | −5.11 | −0.67 | 4.44 |
| | | *E* | 988.5 | −534.0 | 454.5 | 103.0 | −5.22 | −0.68 | 4.54 |
| | | Δ | | | 26.3 | −7.2 | | | |
| **14** |  | *Z* | 981.3 | −513.5 | 467.8 | 110.0 | −5.50 | −0.20 | 5.30 |
| | | *E* | 992.0 | −526.1 | 465.9 | 102.8 | −5.27 | −0.25 | 5.02 |
| | | Δ | | | −1.9 | −7.2 | | | |

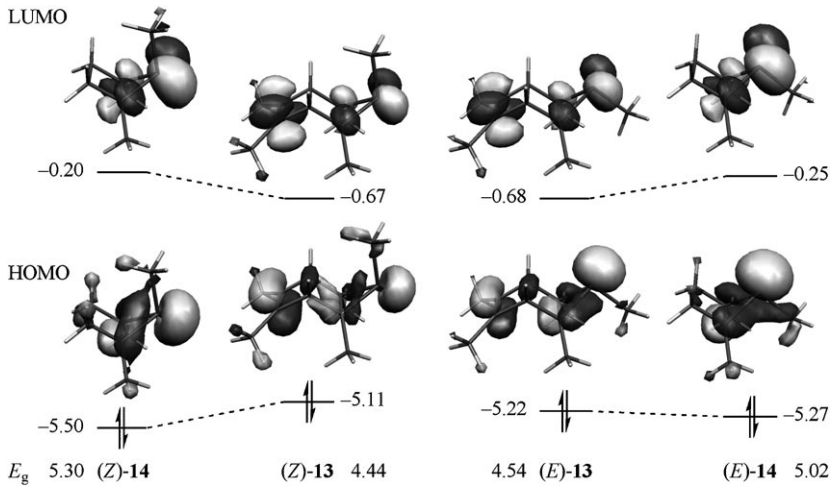


Figure 4. Correlation diagram for (*Z*/*E*)-**14** and **13**, including MO energies and gap energies $E_g$ (eV).

HOMO energies ((*Z*)-**14**: −5.50 vs. **12b′**: −5.99 eV), which leads to smaller energy gaps and, consequently, to stronger paramagnetic deshieldings.

In summary, the low-field $^{31}P$ chemical shift of (*Z*)-**4** as compared to the *E* isomer is caused by 1) the reduced P-pyramidalization of the *Z* isomer due to steric interactions with the central bridge methyl groups and 2) the stronger interaction of the double bond with the phosphorus lone pair in the *Z* isomer.

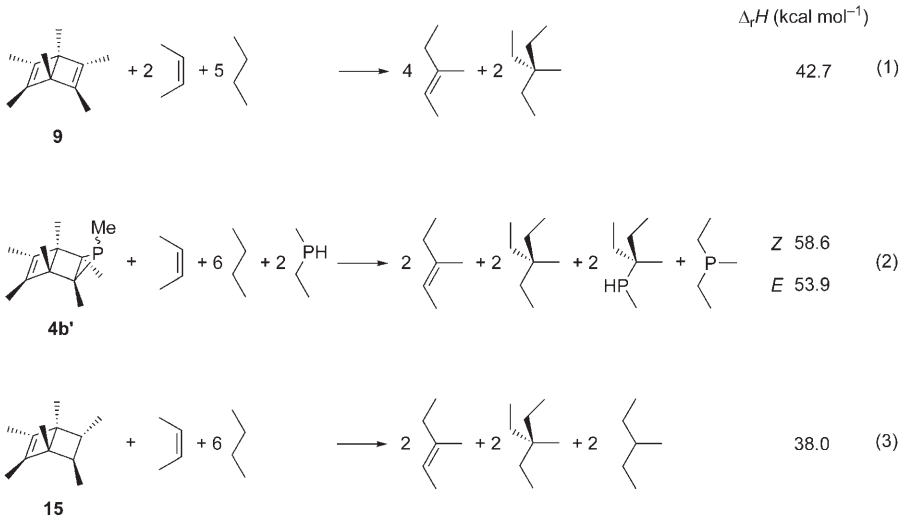


**Ring strain**: For comparison of the ring strain in **4** and **9**, we used the uncomplexed annellated methylphosphirane **4b′** as a model compound. The reaction enthalpies of homodesmotic reactions[24] given in Equations (1)–(3) were calculated at the G3(MP2)//B3LYP/6–31G(d) level of theory.[25,26] The calculated strain energy of 42.7 kcal mol$^{-1}$ for **9** is in excellent agreement with previous experimental estimates of 40–45 kcal mol$^{-1}$,[27] while the annellated phosphirane (*E*)-**4b′** has a larger ring-strain energy of 53.9 kcal mol$^{-1}$. The phosphirane ring apparently introduces 11.2 kcal mol$^{-1}$ extra ring strain, which is, however, half of that calculated for the parent phosphirane $C_2H_4PH$.[24b] The modest contribution of the CCP ring to the strain energy of **4b′** is partly due to the release of 4.7 kcal mol$^{-1}$ of olefin strain in **4b′** [reactions (1) vs. (3)],[28] which compares well with the 5.3 kcal mol$^{-1}$ of olefin strain reported for cyclobutene.[24b,9b]

At this level of theory, (*Z*)-**4b′** is 4.7 kcal mol$^{-1}$ less stable than the (*E*)-**4b′** isomer due to the steric interactions between the P–Me group and the bridgehead methyl groups. For complexed **4**, this energy difference is largely offset by similar interactions with the $W(CO)_5$ group in the *E* isomer. In fact, (*E*)-**4b** is favored over the *Z* isomer by only 0.5 kcal mol$^{-1}$ at the BP86/TZP level.

**Steric congestion of the substrate**: Substrates with two double bonds can give both single and double phosphinidene addition,[9c,29] but only the mono-adducts were obtained in the case of hexamethyl Dewar benzene (HMDB) (**9**). We ascribe this to the steric congestion of the double bonds. When we used, instead of **10**, the "classical" phosphinidene precursor **16** with 10% CuCl as a catalyst ,[30] only 23% conversion to **4a** (*Z*/*E* 5:1) was observed under similar reaction conditions. Several byproducts were formed, most notably diphosphene (15%) and triphosphirane (6%), which are known decomposition products of **16** in the absence of a substrate.[31]

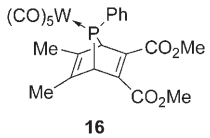


**16**

Reaction at room temperature with a fivefold excess of **9** and 5% CuCl did not improve the conversion. These observations are consistent with the proposed intermediacy of a phosphinidene–CuCl species,[32,8,9b,c] which is sterically more demanding than the "free" phosphinidene complex generated without the $Cu^I$ catalyst. Thermal decomposition of **16** at 110°C with a fivefold excess of **9** afforded a cleaner reaction,[33], but still only 31% conversion to (*Z*)-**4a** was obtained. The small amount of *E* isomer that was also ob-

  

served during the course of the reaction was not stable at the reaction temperature. These results signify the steric congestion in the substrate **9** and the suitability of benzophosphepine **10** as a low-temperature precursor of transient phosphinidene complexes.

**Second cycloaddition**: Products **4a** and **4b** still contained a (hindered) double bond, and we attempted to expand the annellated system with a subsequent cycloaddition (Scheme 2). Reaction of **4a** or **4b** with the corresponding

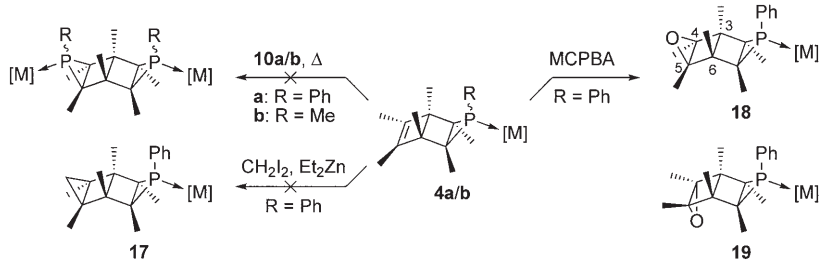


Scheme 2. Reactivity of **4** ([M] = $W(CO)_5$).

benzophosphepine **10** (**a**: 65 °C, **b**: 75 °C) only resulted in decomposition of the precursor.[14b] Clearly, the double bond in **4** is not accessible for phosphinidene addition. The crystal structure of **4a** shows that the central methyl groups (C9 and C12) are tilted toward the double bond, which is in accordance with the observed reduced accessibility.

We reasoned that addition of the smaller singlet methylene $H_2C$: might possibly afford the cyclopropane derivative **17**. The use of the Simmons–Smith carbenoid [$IZnCH_2I$], conveniently generated from diiodomethane and diethylzinc in hexane,[34] was an evident choice. However, whereas **9** was fully converted by excess carbenoid to a mixture of mono- and bis-adduct (**5a** and **6a**, Scheme 3), no addition

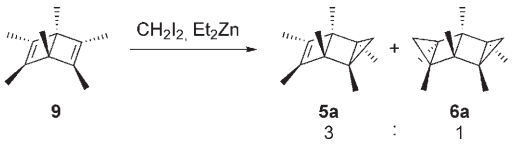


Scheme 3. Methylene addition to **9** with product ratio.

was observed for (*Z*)-**4a**. Instead, epoxidation with *m*-chloroperbenzoic acid (MCPBA), analogous to the generation of **5b** and **6b**[11] was more successful. Thus, reaction of (*Z*)-**4a** with a threefold excess of MCPBA resulted in 42% (by NMR spectroscopy) of tetracyclic **18** ($\delta_P = -69.9$ ppm).[35] The presence of an epoxide ring in complex **18** was established by multinuclear NMR spectroscopy; the spectra indicate that $C_s$ symmetry is retained. In this complex, the vinylic carbon resonance of (*Z*)-**4a** (146.5 ppm) is replaced by one at $\delta = 73.1$ ppm, which is typical for epoxides (compared to **5b**: $\delta = 75.1$ ppm, **6b**: $\delta = 68.6$ ppm[11c]). The presence of an *exo*-epoxide ring, analogous to **5b** and **6b** was corroborated by 2D NOESY measurements. The correlation of the central bridgehead methyl groups (at C3/6) with those at C4/5 (epoxide) is weaker than for the starting material (*Z*)-**4a**. This is consistent with their increased distance in **18**, whereas in *endo*-epoxide **19** these methyl groups would be closer to each other than in (*Z*)-**4a**. Moreover, an interaction is observed between the methyl groups of the phosphirane ring and those of the epoxide ring, which would be absent in **19**. Finally, we calculated $^{31}P$ NMR chemical shifts at the BP86/TZP level[22] for epoxides **18** and **19** of $\delta_{calcd} = -68.7$ and $-88.8$ ppm ($\sigma_{calcd} = 325.9$, 345.9 ppm), respectively. The chemical shift for **18** is in excellent agreement with the experimentally observed $^{31}P$ NMR chemical shift of $\delta = -69.9$ ppm.

## Conclusion

Tricyclic *exo*-phosphiranes **4** have been synthesized by phosphinidene addition to **9**. Benzophosphepine **10** is a suitable phosphinidene precursor for such sterically hindered substrates. The remaining double bond is unreactive toward further 1,2-addition by phosphinidene or methylene species, but can be epoxidized with MCPBA to a tetracyclic P,O-bis-adduct. The large difference in $^{31}P$ NMR chemical shift of (*Z*)- and (*E*)-**4** is found to be due to a combination of steric congestion around the phosphorus atom and electronic interaction of the (coordinated) phosphorus lone pair with the double bond in the *Z* isomer, both of which cause deshielding relative to the *E* isomer. The semiquantitative results of our calculations provide a more systematic understanding of structural influences on $^{31}P$ chemical shieldings. This may pave the way to using $^{31}P$ NMR spectroscopy to monitor structural differences of tailored phosphine ligands in catalysis.

## Experimental Section

**Computation of $^{31}P$ NMR chemical shieldings**: Hybrid density-functional theory geometry optimizations were carried out with ADF 2004.01 at the Becke 88-Perdew 86/TZP level,[22] by using an integration accuracy of 6.0 and convergence criteria of $1 \times 10^{-6}$ for the SCF and $1 \times 10^{-4}$ for the geometry. Subsequently, a single-point SCF calculation was performed with the PBE functional, using a basis set of TZP (4d frozen) for W and ET-pVQZ for all other elements. The resulting wave function and potential were supplied to ADF's EPR/NMR program to calculate the $^{31}P$ chemical shielding. These values are relative to a bare phosphorus nucleus and can be converted to chemical shifts $\delta$ relative to an appropriate reference system, for which we used the phosphirane complex **12b** ($\sigma_{calcd} = 456.4$, $\delta_{exptl} = -199.3$ ppm) to obtain the relationship: $\delta_{calcd}(\text{adduct}) = 257.1 \text{ ppm} - \sigma_{calcd}(\text{adduct})$. Reported shielding contributions are rounded to one, and BP86/TZP MO energies to two decimal places.

**Ring strain analyses**: Structures were optimized with Gaussian 03 (G03)[25] at the B3LYP/6–31G(d) level of theory by using tight SCF and

  

geometry convergence criteria and an ultrafine integration grid and were verified as minima by frequency calculations. The strain energies were determined by calculating the G3(MP2)//B3LYP/6–31G(d) enthalpies at 298.15 K for the homodesmotic reactions. The size of (*Z*/*E*)-**4b′** required the use of a 64 bits implementation of G03.

**General**: All reactions were carried out under nitrogen using standard Schlenk techniques. Hexamethyl Dewar benzene (**9**), dichloromethane (DCM), and 70% *m*-chloroperbenzoic acid (MCPBA) were used as received. Diethylzinc was purchased as a 1.0 M solution in hexanes. Toluene was distilled over sodium. The syntheses of benzophosphepines **10a** and **10b** have been described elsewhere.[14] NMR measurements were performed (at 298 K) on a Bruker Avance 250 ($^{1}$H, $^{13}$C, $^{31}$P) or a Bruker Avance 400 ($^{1}$H, $^{13}$C, 2D spectra). NMR chemical shifts were internally referenced to the solvent for $^{1}$H ($CHCl_3$: $\delta = 7.26$ ppm, $C_6HD_5$: $\delta = 7.16$ ppm) and $^{13}$C ($CDCl_3$: $\delta = 77.16$ ppm, $C_6D_6$: $\delta = 128.06$ ppm),[36] and externally for $^{31}$P to 85% $H_3PO_4$. Infrared (IR) spectra were recorded on a Mattson-6030 Galaxy Series FTIR spectrometer, and GC–MS spectra on a HP 5890 Series II GC (column BP5 25 m, 0.25 mm ID) with a HP 5971 Series MS unit. High-resolution mass spectra (HR-MS) were measured on a Finnigan Mat 900 mass spectrometer operating at an ionization potential of 70 eV. The elemental analysis of (*Z*)-**4a** was performed by the Microanalytical Laboratory of the Laboratorium für Organische Chemie, ETH Zürich. Melting points were measured on samples in unsealed capillaries and are uncorrected.

**(Hexamethyl-3-phenyl-3-phosphatricyclo[3.2.0.0$^{2,4}$]hept-6-en-3-yl)pentacarbonyltungsten (4a)**

*Procedure A*: **10a** (125.95 mg, 225 μmol) and **9** (90.9 μL, 450 μmol) were dissolved in toluene (2.25 mL), and heated to 55 °C for 4.5 days. $^{31}$P NMR spectroscopy showed complete conversion to **4a** (*Z*/*E* 1.1:1). Volatiles were evaporated and the crude product was purified by column chromatography over silica gel eluted with pentane, which yielded a white solid (80.8 mg, 136 μmol, 60%). The *Z* isomer could be separated from the *E* by column chromatography over silica gel eluted with 19:1 pentane/DCM, followed by fractional crystallization from hexane at −20 °C.

(*Z*)-**4a**: Colorless crystalline solid, m.p. = 145 °C (decomp); $R_f$ (silica/pentane): 0.30; $^{1}$H NMR (250.1 MHz, $CDCl_3$): $\delta = 7.54$ (ddd, $^{3}J_{HP} = 10.8$, $^{3}J_{HH} = 7.8$, $^{4}J_{HH} = 1.6$ Hz, 2H; *o*-PhH), 7.38–7.26 (m, 3H; *m*/*p*-PhH), 1.68 (d, $^{5}J_{HP} = 0.9$ Hz, 6H; =CMe), 1.51 (d, $^{3}J_{HP} = 16.4$ Hz, 6H; PCMe), 0.84 ppm (s, 6H; PCCMe); $^{13}$C{$^{1}$H} NMR (100.6 MHz, $CDCl_3$): $\delta = 199.7$ (d, $^{2}J_{CP} = 27.2$ Hz, $CO_{ax}$), 196.7 (d, $^{2}J_{CP} = 7.9$ Hz, $CO_{eq}$), 146.5 (d, $^{3}J_{CP} = 4.6$ Hz, =C), 137.6 (d, $^{1}J_{CP} = 17.2$ Hz, *ipso*-Ph), 133.1 (d, $^{2}J_{CP} = 11.3$ Hz, *o*-Ph), 129.6 (d, $^{4}J_{CP} = 2.0$ Hz, *p*-Ph), 127.9 (d, $^{3}J_{CP} = 9.4$ Hz, *m*-Ph), 54.3 (d, $^{2}J_{CP} = 7.8$ Hz, PC*C*), 49.3 (d, $^{1}J_{CP} = 18.0$ Hz, PC), 15.5 (d, $^{2}J_{CP} = 10.3$ Hz, PC*Me*), 11.4 (d, $^{3}J_{CP} = 2.9$ Hz, PCC*Me*), 11.0 ppm (s, =C*Me*); $^{31}$P{$^{1}$H} NMR (101.3 MHz, $CDCl_3$): $\delta = -63.0$ ppm ($^{1}J_{PW} = 250.3$ Hz); IR (KBr): $\tilde{\nu} = 2069.5$ (m, $CO_{ax}$), 1928.5, 1910.8 cm$^{-1}$ (br s, $CO_{eq}$); HR-MS: calcd for $C_{23}H_{23}O_5PW$: 594.0793; found: 594.0795; *m*/*z* (%): 594 (2) [*M*]$^+$, 510 (1) [*M*−3CO]$^+$, 482 (1) [*M*−4CO]$^+$, 454 (36) [*M*−5CO]$^+$, 452 (41), 432 (14) [*M*−**9**]$^+$, 404 (100) [*M*−**9**−CO]$^+$, 376 (18) [*M*−**9**−2CO]$^+$, 348 (92) [*M*−**9**−3CO]$^+$, 320 (31) [*M*−**9**−4CO]$^+$, 292 (31) [*M*−**9**−5CO]$^+$, 161 (15) [hexamethyl benzene (HMB)−H]$^+$, 147 (37) [HMB−Me]$^+$; elemental analysis calcd (%) for $C_{23}H_{23}O_5PW$: C 46.49, H 3.90; found: C 46.62, H 3.97. (*E*)-**4a**: $R_f$ (silica/pentane): 0.25; $^{1}$H NMR (400.1 MHz, $CDCl_3$): $\delta = 7.37$ (td, $^{3}J_{HH} = 7.4$, $^{4}J_{HP} = 2.5$ Hz, 2H; *m*-PhH), 7.31–7.25 (m, 3H; *o*/*p*-PhH), 1.68 (d, $^{5}J_{HP} = 1.2$ Hz, 6H; =CMe), 1.29 (s, 6H; PCCMe), 1.27 ppm (d, $^{3}J_{HP} = 10.2$ Hz, 6H; PCMe); $^{13}$C{$^{1}$H} NMR (100.6 MHz, $CDCl_3$): $\delta = 199.2$ (d, $^{2}J_{CP} = 30.5$ Hz, $CO_{ax}$), 197.5 (d, $^{2}J_{CP} = 7.6$ Hz, $CO_{eq}$), 143.2 (d, $^{3}J_{CP} = 6.7$ Hz, =C), 139.6 (d, $^{1}J_{CP} = 28.0$ Hz, *ipso*-Ph), 132.8 (d, $^{2}J_{CP} = 9.2$ Hz, *o*-Ph), 129.1 (d, $^{4}J_{CP} = 1.1$ Hz, *p*-Ph), 128.9 (d, $^{3}J_{CP} = 8.3$ Hz, *m*-Ph), 55.1 (d, $^{2}J_{CP} = 4.7$ Hz, PC*C*), 44.9 (d, $^{1}J_{CP} = 15.5$ Hz, PC), 13.3 (s, PCC*Me*), 12.2 (d, $^{3}J_{CP} = 7.2$ Hz, PC*Me*), 10.8 ppm (s, =C*Me*); $^{31}$P{$^{1}$H} NMR (101.3 MHz, $CDCl_3$): $\delta = -126.9$ ppm ($^{1}J_{PW} = 241.5$ Hz).

*Procedure B*: CuCl (1.2 mg, 12 μmol, 10%), complex **16a** (81.4 mg, 137 μmol), and **9** (24.5 μL, 121 μmol) were heated in toluene (0.4 mL) at 50 °C for 4.5 h. $^{31}$P NMR spectroscopy of the resulting intense red mixture indicated 23% conversion to **4a** (*Z*/*E* 5:1), along with diphosphene (15%, $\delta_P = -18$ ppm ($^{1}J_{PW} = 139$, $^{1}J_{PW} = 103$, $^{2}J_{PW} = 32$ Hz)), triphosphirane (6%, $\delta_P = -92$ (dd, $^{1}J_{PP} = 215$, $^{1}J_{PP} = 176$ Hz), −119 (dd, $^{1}J_{PP} = 176$, $^{1}J_{PP} = 165$ Hz), −129 ppm (dd, $^{1}J_{PP} = 215$, $^{1}J_{PP} = 165$ Hz)), and small amounts of other unidentified byproducts.

*Procedure C*: CuCl (0.6 mg, 6 μmol, 5%), complex **16a** (79.5 mg, 122 μmol), and **9** (125 μL, 619 μmol) were stirred in toluene (1.5 mL) at room temperature for 10 days. $^{31}$P NMR spectroscopy of the resulting intense red mixture indicated 24% conversion to **4a** (*Z*/*E* 8:1).

*Procedure D*: Complex **16a** (37.3 mg, 57 μmol) and **9** (58 μL, 287 μmol) were dissolved in toluene (0.50 mL), and heated to 110 °C for 20 h. Conversion to **4a** was determined by $^{31}$P NMR spectroscopy: 26% after 4 h (*Z*/*E* 7:1), 31% after 20 h (only *Z*).

**(Heptamethyl-3-phosphatricyclo[3.2.0.0$^{2,4}$]hept-6-en-3-yl)pentacarbonyltungsten (4b)**: Compound **10b** (299 mg, 0.60 mmol) and **9** (303 μL, 1.50 mmol) were dissolved in toluene (5.0 mL) and heated to 65 °C for 6 days. $^{31}$P NMR spectroscopy showed complete conversion to **4b** (*Z*/*E* 1.4:1) with traces of byproduct at $\delta = -21.0$ and −125.7 (d, $J = 13.7$ Hz), −23.4 and −150.7 ppm (d, $J = 14.4$ Hz), which we ascribed to decomposition products of **10b** in analogy with **10a**.[14b] Volatiles were evaporated and the crude product was purified by column chromatography over silica gel eluted with 19:1 pentane/toluene. The obtained off-white solid (0.211 g, 0.40 mmol, 66%) also contained 8% hexamethyl benzene, but we were unable to remove this impurity by column chromatography and crystallization. *Z* and *E* enriched fractions were obtained by preparative thin-layer chromatography eluted with 1% diethyl ether (DEE) in pentane. (*Z*)-**4b**: $R_f$ (silica/pentane): 0.40; $^{1}$H NMR (400.1 MHz, $C_6D_6$): $\delta = 1.37$ (d, $^{5}J_{HP} = 0.9$ Hz, 6H; =CMe), 1.35 (d, $^{2}J_{HP} = 7.0$ Hz, 3H; PMe), 1.17 (d, $^{3}J_{HP} = 15.8$ Hz, 6H; PCMe), 0.75 ppm (s, 6H; PCCMe); $^{13}$C{$^{1}$H} NMR (100.6 MHz, $C_6D_6$): $\delta = 198.7$ (d, $^{2}J_{CP} = 26.2$ Hz, $CO_{ax}$), 197.0 (d, $^{2}J_{CP} = 8.0$ Hz, $CO_{eq}$), 144.2 (d, $^{3}J_{CP} = 4.7$ Hz, =C), 55.9 (d, $^{2}J_{CP} = 6.9$ Hz, PC*C*), 45.7 (d, $^{1}J_{CP} = 14.1$ Hz, PC), 16.1 (d, $^{1}J_{CP} = 4.7$ Hz, PMe), 14.1 (d, $^{2}J_{CP} = 9.5$ Hz, PC*Me*), 12.8 (d, $^{3}J_{CP} = 3.0$ Hz, PCC*Me*), 10.4 ppm (s, =CMe); $^{31}$P{$^{1}$H} NMR (101.3 MHz, $C_6D_6$): $\delta = -87.1$ ppm ($^{1}J_{PW} = 249.2$ Hz).

(*E*)-**4b**: $R_f$ (silica/pentane): 0.35; $^{1}$H NMR (400.1 MHz, $C_6D_6$): $\delta = 1.40$ (d, $^{5}J_{HP} = 1.3$ Hz, 6H; =CMe), 1.14 (s, 6H; PCCMe), 0.89 (d, $^{3}J_{HP} = 9.9$ Hz, 6H; PCMe), 0.86 ppm (d, $^{2}J_{HP} = 5.4$ Hz, 3H; PMe); $^{13}$C{$^{1}$H} NMR (100.6 MHz, $C_6D_6$): $\delta = 198.5$ (d, $^{2}J_{CP} = 28.7$ Hz, $CO_{ax}$), 198.0 (d, $^{2}J_{CP} = 7.7$ Hz, $CO_{eq}$), 143.3 (d, $^{3}J_{CP} = 6.7$ Hz, =C), 54.1 (d, $^{2}J_{CP} = 4.0$ Hz, PC*C*), 43.1 (d, $^{1}J_{CP} = 11.1$ Hz, PC), 16.7 (d, $^{1}J_{CP} = 15.8$ Hz, PMe), 11.7 (d, $^{3}J_{CP} = 6.6$ Hz, PCC*Me*), 10.5 (s, =C*Me*), 9.80 ppm (s, PC*Me*); $^{31}$P{$^{1}$H} NMR (101.3 MHz, $C_6D_6$): $\delta = -138.2$ ($^{1}J_{PW} = 241.1$ Hz); HR-MS: calcd for $C_{18}H_{21}O_5PW$: 532.06359; found: 532.06547; *m*/*z* (%): 532 (4) [*M*]$^+$, 504 (2) [*M*−CO]$^+$, 476 (1) [*M*−2CO]$^+$, 448 (2) [*M*−3CO]$^+$, 433 (5) [*M*−Me−3CO]$^+$, 390 (8), 377 (9) [*M*−Me−6CO]$^+$, 370 (11) [*M*−**9**]$^+$, 342 (41) [*M*−**9**−CO]$^+$, 314 (12) [*M*−**9**−2CO]$^+$, 286 (7) [*M*−**9**−3CO]$^+$, 258 (4) [*M*−**9**−4CO]$^+$, 162 (56) [HMB]$^+$, 147.1 (100) [HMB−Me]$^+$.

**(1-Methylphosphiran-1-yl)pentacarbonyltungsten (12b)**:[18] Compound **16b** (100 mg, 0.17 mmol) in toluene (2 mL) was transferred to a 5 mL pressure chamber. A suspension of a small amount of CuCl in toluene (1 mL) was added and the channel was rinsed with of toluene (1 mL). Ethylene pressure (65 bar) was applied and the solution was stirred overnight at 40 °C, after which time the yellow color had paled. The solution was removed from the chamber; the solvent was evaporated, and the light brown residue was purified by chromatography and sublimation to give a white solid (50 mg, 0.13 mmol, 74%). $^{1}$H NMR ($CDCl_3$): $\delta = 1.38$ (d, $^{2}J_{HP} = 7.5$ Hz, 3H; PMe), 1.09–1.35 (m, 4H; $CH_2$); $^{13}$C NMR ($CDCl_3$): $\delta = 196.0$ (d, $^{2}J_{CP} = 8.4$ Hz, $CO_{eq}$), 17.3 (d, $^{1}J_{CP} = 15.8$ Hz, PMe), 9.1 ppm (d, $^{1}J_{CP} = 10.8$ Hz, $CH_2$), $CO_{ax}$ could not be observed; $^{31}$P NMR ($CDCl_3$): $\delta = -199.3$ ppm ($^{1}J_{PW} = 254.1$ Hz); IR (KBr): $\tilde{\nu} = 2074.3$ (m, $CO_{ax}$), 1929.7 (s, $CO_{eq}$), 1101.3 (w), 1023.2 (w), 948.0 (w), 597.9 (w), 572.8 cm$^{-1}$ (w); HR-MS: calcd for $C_8H_7PO_5W$: 397.95410; found: 397.95462; *m*/*z* (%): 398 (45) [*M*]$^+$, 370 (8) [*M*−CO]$^+$, 286 (100) [*M*−4CO]$^+$, 256 (76), 228 (56), 43 (86).

**Methylene addition to 9**: Diethylzinc (2.48 mL, 2.48 mmol) was added to **9** (100 μL, 495 μmol) in hexane (10 mL) at 0 °C. Diiodomethane (166 μL, 1.98 mmol) was added dropwise under formation of a white precipitate. The mixture was warmed to 45 °C for 3 days, then purified by extraction with an aqueous saturated ammonium chloride solution. GC–MS analysis (injector 140 °C; oven 40–230 °C at 5–14.5 min) showed no trace of the starting material. A mixture of mono- and bis-adduct (3:1) was obtained

  

as a colorless oil (76 mg, 85%). The spectroscopic data of the adducts are consistent with those reported in the literature.[10a,c]

**Mono-adduct 5a**: $^1$H NMR (250.1 MHz, $CDCl_3$): $\delta=1.62$ (s, 6H; =CMe), 1.08 (s, 6H; $CH_2CMe$), 0.80 (s, 6H; $CH_2CCMe$), 0.89, 0.25 ppm (d, 2H; $^2J_{HH}=-4.3$ Hz, $CH_2$); $^{13}$C{$^1$H} NMR (62.9 MHz, $CDCl_3$): $\delta=143.3$ (=C), 53.0 ($CH_2CC$), 36.6 ($CH_2C$), 28.5 ($CH_2$), 12.8 ($CH_2CMe$), 11.1 ($CH_2CCMe$), 10.3 ppm (=$CMe$); GC–MS ($t=12.75$ min) $m/z$ (%): 176 (4) $[M]^+$, 161 (100) $[M-Me]^+$, 146 (8) $[M-2Me]^+$, 133 (39), 119 (41), 107 (52), 105 (39), 91 (49), 79 (17), 77 (24), 65 (12), 63 (7), 53 (16), 51 (13), 41 (23), 39 (35).

**Bis-adduct 6a**: $^1$H NMR (250.1 MHz, $CDCl_3$): $\delta=1.30$ (s, 12H; $CH_2CMe$), 0.64 (s, 6H; $CH_2CCMe$), 0.54, −0.15 ppm (d, 4H; $^2J_{HH}=-3.6$ Hz, $CH_2$); $^{13}$C{$^1$H} NMR (62.9 MHz, $CDCl_3$): $\delta=52.1$ ($CH_2CC$), 32.3 ($CH_2C$), 27.3 ($CH_2$), 13.5 ($CH_2CMe$), 11.4 ppm ($CH_2CCMe$); GC–MS ($t=14$ min) $m/z$ (%): 190 (1) $[M]^+$, 175 $[M-Me]^+$, 161 (11), 147 (31), 133 (100), 119 (67), 105 (50), 93 (17), 91 (61), 79 (24), 77 (31), 67 (11), 65 (15), 53 (26), 41 (41), 39 (45).

**Attempted phosphinidene addition to 4a**: Compounds **10a** (17.04 mg, 30.4 μmol) and (*Z*)-**4a** (14.63 mg, 24.6 μmol) were dissolved in toluene (0.50 mL) and heated to 65°C for 3 h. $^{31}$P NMR spectroscopy showed only unreacted (*Z*)-**4a** and decomposition products of **10a** at $\delta=-7.2$ and −119.9 (d, $J=11.8$ Hz), −8.7 and −128.2 (d, $J=14.3$ Hz), −15.9 and −123.7 ppm (d, $J=11.5$ Hz).[14b]

**Attempted phosphinidene addition to 4b**: Compounds **10b** (12.43 mg, 25.0 μmol) and **4b** (14.27 mg, 26.8 μmol) were dissolved in toluene (0.50 mL), and heated to 75°C for 3 h. $^{31}$P NMR spectroscopy showed only unreacted **4b** and signals at $\delta=-22.7$ and −127.4 (d, $J=13.7$ Hz), −25.0 and −152.4 ppm (d, $J=14.5$ Hz), which we ascribed to the decomposition products of **10b** analogous to **10a**.[14b]

**Attempted methylene addition to 4a**: Diethylzinc (0.10 mL, 100 μmol) was added to (*Z*)-**4a** (11.95 mg, 20.1 μmol) in hexane (1.0 mL) at 0°C. Diiodomethane (6.6 μL, 81.6 μmol) was added slowly under the formation of a white precipitate. The mixture was stirred at 25°C for one week, then purified by using an aqueous saturated ammonium chloride solution. $^{31}$P and $^1$H NMR spectroscopy showed only unreacted (*Z*)-**4a**.

**Epoxidation of 4a**: MCPBA (10 mg, 41 μmol) in DCM (3 mL) was dried over magnesium sulfate, filtered, and added dropwise to a solution of (*Z*)-**4a** (7.8 mg, 13 μmol) in DCM (2 mL) at 0°C. After 15 min, the mixture was stirred for 30 min at 25°C. The modest stability of the $W(CO)_5$ moiety in DCM precludes extensive reaction times. After evaporation, the faintly yellow residue was redissolved in pentane and washed five times with water (≈3 mL). Evaporation of the solvent afforded a white solid (6.9 mg), which consisted of 47% unreacted (*Z*)-**4a**, 42% **18**, and 11% of an unidentified byproduct at $\delta_P=45.8$ ppm. Data for compound **18**: $^1$H NMR (400.1 MHz, $C_6D_6$): $\delta=7.28$ (ddd, $^3J_{HP}=10.9$, $^3J_{HH}=7.4$, $^4J_{HH}=1.9$ Hz, 2H; *o*-PhH), 6.89–6.82 (m, 3H; *m*/*p*-PhH), 1.42 (d, $^3J_{HP}=17.2$ Hz, 6H; PCMe), 1.28 (s, 6H; OCMe), 0.76 ppm (s, 6H; PCCMe); $^{13}$C{$^1$H} NMR (100.6 MHz, $C_6D_6$): $\delta=196.7$ (d, $^2J_{CP}=8.0$ Hz, $CO_{eq}$), 137.3 (d, $^1J_{CP}=17.6$ Hz, *ipso*-Ph), 133.3 (d, $^2J_{CP}=11.8$ Hz, *o*-Ph), 130.0 (d, $^4J_{CP}=2.0$ Hz, *p*-Ph), 127.9 (*m*-Ph, buried under the solvent signal), 73.1 (d, $^3J_{CP}=5.9$ Hz, OC), 60.6 (d, $^2J_{CP}=7.3$ Hz, PC*C*), 45.2 (d, $^1J_{CP}=16.3$ Hz, PC), 16.0 (d, $^2J_{CP}=10.7$ Hz, PC*Me*), 11.8 (s, OC*Me*), 11.3 ppm (d, $^3J_{CP}=3.4$ Hz, PCC*Me*), $CO_{ax}$ could not be observed; $^{31}$P{$^1$H} NMR (101.3 MHz, $C_6D_6$): $\delta=-69.9$ ppm ($^1J_{PW}=260.1$ Hz); HR–MS: calcd for $C_{23}H_{23}O_6PW$: 610.0742; found: 610.0712.

**Crystal data for (*Z*)-4a**: $C_{23}H_{23}O_5PW$, $M_r=594.23$, colorless needle, 0.48×0.18×0.03 mm, triclinic, $P\bar{1}$ (no. 2), $a=7.62343(14)$, $b=11.8399(3)$, $c=13.0811(3)$ Å, $\alpha=77.816(1)$, $\beta=82.605(1)$, $\gamma=85.718(1)$°, $V=1143.14(4)$ Å$^3$, $Z=2$, $\rho_{calcd}=1.726$ g cm$^{-3}$, $\mu=5.15$ mm$^{-1}$. 25262 reflections were measured on a Nonius KappaCCD diffractometer with rotating anode (graphite monochromator, $\lambda=0.71073$ Å) up to a resolution of $(\sin\theta/\lambda)_{max}=0.65$ Å$^{-1}$ at a temperature of 150 K. Intensities were integrated with EvalCCD[37] by using an accurate description of the experimental setup for the prediction of the reflection contours. An absorption correction based on multiple measured reflections was applied using the program SADABS[38] (0.44–0.86 correction range). 5230 reflections were unique ($R_{int}=0.0285$). The structure was solved with the program DIRDIF-99[39] using automated Patterson Methods and refined with SHELXL-97[40] against $F^2$ of all reflections. Non-hydrogen atoms were refined with anisotropic displacement parameters. All hydrogen atoms were introduced in calculated positions and refined with a riding model. 277 parameters were refined with no restraints. $R1/wR2$ [$I>2\sigma(I)$]: 0.0190/0.0407. $R1/wR2$ (all data): 0.0228/0.0419. $S=1.040$. Residual electron density between −1.17 and 1.77 e Å$^{-3}$. Molecular illustration, geometry calculations, and checking for higher symmetry were performed with the PLATON program.[41] CCDC 636374 contains the supplementary crystallographic data for this paper. These data can be obtained free of charge from The Cambridge Crystallographic Data Centre via www.ccdc.cam.ac.uk/data_request/cif..

## Acknowledgement

This work was supported by the Netherlands Organization for Scientific Research, Chemical Sciences (NWO-CW). We acknowledge the National Center for Computing Facilities (SARA) and NWO/NCF for computer time. We thank Dr. M. Smoluch for measuring the high-resolution mass spectra and Ing. T. Nijbacker for the synthesis of phosphirane **12b**. We are indebted to one of the referees for constructive comments.

[1] a) T. T. Derencsényi, *Inorg. Chem.* **1981**, *20*, 665–670; b) M. Ackermann, A. Pascariu, T. Höcher, H.-U. Siehl, S. Berger, *J. Am. Chem. Soc.* **2006**, *128*, 8434–8440.

[2] a) A. Dransfeld, P. von R. Schleyer, *Magn. Reson. Chem.* **1998**, *36*, S29-S43; b) L. D. Quin, *A Guide to Organophosphorus Chemistry*, Wiley, New York, **2000**, chapter 6, pp. 169–203.

[3] a) L. D. Quin, K. C. Caster, J. C. Kisalus, K. A. Mesch, *J. Am. Chem. Soc.* **1984**, *106*, 7021–7032; b) E. Lindner, R. Fawzi, H. A. Mayer, K. Eichele, W. Hiller, *Organometallics* **1992**, *11*, 1033–1043; c) L. D. Quin, G. Keglevich, A. S. Ionkin, R. Kalgutkar, G. Szalontai, *J. Org. Chem.* **1996**, *61*, 7801–7807.

[4] a) D. B. Chesnut, L. D. Quin, K. D. Moore, *J. Am. Chem. Soc.* **1993**, *115*, 11984–11990; b) D. B. Chesnut, *Chem. Phys.* **1997**, *224*, 133–141; c) D. B. Chesnut, L. D. Quin, S. B. Wild, *Heteroat. Chem.* **1997**, *8*, 451–457; d) D. B. Chesnut, L. D. Quin, *Heteroat. Chem.* **1999**, *10*, 566–572.

[5] a) Y. Ruiz-Morales, T. Ziegler, *J. Phys. Chem. A* **1998**, *102*, 3970–3976; b) G. M. Bernard, G. Wu, M. D. Lumsden, R. E. Wasylishen, N. Maigrot, C. Charrier, F. Mathey, *J. Phys. Chem. A* **1999**, *103*, 1029–1037; c) C. van Wüllen, *Phys. Chem. Chem. Phys.* **2000**, *2*, 2137–2144; d) K. W. Feindel, R. E. Wasylishen, *Can. J. Chem.* **2004**, *82*, 27–44.

[6] a) F. Mathey, *Angew. Chem.* **1987**, *99*, 285–296; *Angew. Chem. Int. Ed. Engl.* **1987**, *26*, 275–286; b) *Multiple Bonds and Low Coordination in Phosphorus Chemistry* (Eds.: M. Regitz, O. J. Scherer), Thieme, Stuttgart, **1991**; c) K. B. Dillon, F. Mathey, J. F. Nixon, *Phosphorus: The Carbon Copy*, Wiley, New York, **1998**; d) F. Mathey, N. H. T. Huy, A. Marinetti, *Helv. Chim. Acta* **2001**, *84*, 2938–2957; e) K. Lammertsma, M. J. M. Vlaar, *Eur. J. Org. Chem.* **2002**, 1127–1138; f) K. Lammertsma, *Top. Curr. Chem.* **2003**, *229*, 95–119.

[7] J.-T. Hung, P. Chand, F. R. Fronczek, S. F. Watkins, K. Lammertsma, *Organometallics* **1993**, *12*, 1401–1405.

[8] J. C. Slootweg, S. Krill, F. J. J. de Kanter, M. Schakel, A. W. Ehlers, M. Lutz, A. L. Spek, K. Lammertsma, *Angew. Chem.* **2005**, *117*, 6737–6740; *Angew. Chem. Int. Ed.* **2005**, *44*, 6579–6582.

[9] a) M. J. M. Vlaar, M. H. Lor, A. W. Ehlers, M. Schakel, M. Lutz, A. L. Spek, K. Lammertsma, *J. Org. Chem.* **2002**, *67*, 2485–2493; b) J. C. Slootweg, F. J. J. de Kanter, M. Schakel, A. W. Ehlers, S. I. Kozhushkov, A. de Meijere, M. Lutz, A. L. Spek, K. Lammertsma, *J. Am. Chem. Soc.* **2004**, *126*, 3050–3051; c) J. C. Slootweg, F. J. J. de Kanter, M. Schakel, M. Lutz, A. L. Spek, S. I. Kozhushkov, A. de Meijere, K. Lammertsma, *Chem. Eur. J.* **2005**, *11*, 6982–6993.

  

[10] a) E. Müller, H. Kessler, *Tetrahedron Lett.* **1968**, *9*, 3037–3040; b) H. Prinzbach, E. Druckrey, *Tetrahedron Lett.* **1968**, *9*, 4285–4288; c) S. D. Reilly, C. C. Wamser, *J. Org. Chem.* **1991**, *56*, 5232–5234.
[11] a) T. G. Traylor, A. R. Miksztal, *J. Am. Chem. Soc.* **1987**, *109*, 2270–2274; b) A. Dunand, R. Gerdil, *Acta Crystallogr. Sect. B* **1980**, *36*, 472–474; c) A. Asouti, L. P. Hadjiarapoglou, *Tetrahedron Lett.* **2000**, *41*, 539–542.
[12] M. G. Barlow, R. N. Haszeldine, W. D. Morton, D. R. Woodward, *J. Chem. Soc. Perkin Trans. 1* **1973**, 1798–1802.
[13] J. M. Bolster, H. Hogeveen, R. M. Kellogg, L. Zwart, *J. Am. Chem. Soc.* **1981**, *103*, 3955–3956.
[14] a) M. L. G. Borst, R. E. Bulo, C. Winkel, D. J. Gibney, A. W. Ehlers, M. Schakel, M. Lutz, A. L. Spek, K. Lammertsma, *J. Am. Chem. Soc.* **2005**, *127*, 5800–5801; b) M. L. G. Borst, R. E. Bulo, D. J. Gibney, Y. Alem, F. J. J. de Kanter, A. W. Ehlers, M. Schakel, M. Lutz, A. L. Spek, K. Lammertsma, *J. Am. Chem. Soc.* **2005**, *127*, 16985–16999.
[15] We have adopted the numbering scheme from the crystal structure of (*Z*)-**4a** in Figure 2, rather than the formal numbering for fused ring systems.
[16] a) See: T. T. Tidwell, T. G. Traylor, *J. Org. Chem.* **1968**, *33*, 2614–2620, and references therein; b) S. Inagaki, H. Fujimoto, K. Fukui, *J. Am. Chem. Soc.* **1976**, *98*, 4054–4061; c) R. Huisgen, P. H. J. Ooms, M. Mingin, N. L. Allinger, *J. Am. Chem. Soc.* **1980**, *102*, 3951–3953.
[17] a) N. H. T. Huy, F. Mathey, *Phosphorus Sulfur Silicon Relat. Elem.* **1990**, *47*, 477–481; b) J.-T. Hung, S.-W. Yang, G. M. Gray, K. Lammertsma, *J. Org. Chem.* **1993**, *58*, 6786–6790.
[18] M. L. G. Borst, *Generating Phosphinidenes: New Approaches*, PhD Thesis, Vrije Universiteit, Amsterdam (The Netherlands), **2005**, Chapter 2.
[19] J.-T. Hung, S.-W. Yang, P. Chand, G. M. Gray, K. Lammertsma, *J. Am. Chem. Soc.* **1994**, *116*, 10966–10971.
[20] a) H. Irngartinger, T. Oeser, R. Jahn, D. Kallfass, *Chem. Ber.* **1992**, *125*, 2067–2073; b) R. Gleiter, F. Ohlbach, T. Oeser, H. Irngartinger, *Liebigs Ann.* **1996**, 785–790.
[21] The acute interplanar angles of the central cyclobutane ring with the phosphirane and the cyclobutene ring are 61.43(19)° and 69.78(19)°, respectively. C9 and C12 make acute interplanar angles of 49.6(2)° with the central cyclobutane and 60.7(2)° with the cyclobutene ring.
[22] a) "Chemistry with ADF": G. te Velde, F. M. Bickelhaupt, E. J. Baerends, C. Fonseca Guerra, S. J. A. van Gisbergen, J. G. Snijders, T. Ziegler, *J. Comput. Chem.* **2001**, *22*, 931–967; b) C. Fonseca Guerra, J. G. Snijders, G. te Velde, E. J. Baerends, *Theor. Chem. Acc.* **1998**, *99*, 391–403; c) ADF2004.01, SCM, Theoretical Chemistry, Vrije Universiteit, Amsterdam (The Netherlands), http://www.scm.com.
[23] *Calculation of NMR and EPR Parameters—Theory and Applications* (Eds: M. Kaupp, M. Bühl, V. G. Malkin), Wiley-VCH, Weinheim, **2004**.
[24] a) P. George, M. Trachtman, C. W. Bock, A. M. Brett, *Tetrahedron* **1976**, *32*, 317–323; b) T. P. M. Goumans, A. W. Ehlers, K. Lammertsma in *Encyclopedia of Computational Chemistry* (Ed: P. von R. Schleyer), Wiley, New York, **2004**, published on the web (http://www.mrw.interscience.wiley.com/ecc/articles/cn0067/frame.html); c) M. L. G. Borst, A. W. Ehlers, K. Lammertsma, *J. Org. Chem.* **2005**, *70*, 8110–8116.
[25] Gaussian 03 (Revisions B.05 and C.02), M. J. Frisch, G. W. Trucks, H. B. Schlegel, G. E. Scuseria, M. A. Robb, J. R. Cheeseman, J. A. Montgomery, Jr., T. Vreven, K. N. Kudin, J. C. Burant, J. M. Millam, S. S. Iyengar, J. Tomasi, V. Barone, B. Mennucci, M. Cossi, G. Scalmani, N. Rega, G. A. Petersson, H. Nakatsuji, M. Hada, M. Ehara, K. Toyota, R. Fukuda, J. Hasegawa, M. Ishida, T. Nakajima, Y. Honda, O. Kitao, H. Nakai, M. Klene, X. Li, J. E. Knox, H. P. Hratchian, J. B. Cross, V. Bakken, C. Adamo, J. Jaramillo, R. Gomperts, R. E. Stratmann, O. Yazyev, A. J. Austin, R. Cammi, C. Pomelli, J. W. Ochterski, P. Y. Ayala, K. Morokuma, G. A. Voth, P. Salvador, J. J. Dannenberg, V. G. Zakrzewski, S. Dapprich, A. D. Daniels, M. C. Strain, O. Farkas, D. K. Malick, A. D. Rabuck, K. Raghavachari, J. B. Foresman, J. V. Ortiz, Q. Cui, A. G. Baboul, S. Clifford, J. Cioslowski, B. B. Stefanov, G. Liu, A. Liashenko, P. Piskorz, I. Komaromi, R. L. Martin, D. J. Fox, T. Keith, M. A. Al-Laham, C. Y. Peng, A. Nanayakkara, M. Challacombe, P. M. W. Gill, B. Johnson, W. Chen, M. W. Wong, C. Gonzalez, J. A. Pople, Gaussian, Inc., Wallingford CT, **2004**.
[26] A. G. Baboul, L. A. Curtiss, P. C. Redfern, *J. Chem. Phys.* **1999**, *110*, 7650–7657.
[27] a) J. F. M. Oth, *Recl. Trav. Chim. Pays-Bas* **1968**, *87*, 1185–1195; b) W. Adam, J. C. Chang, *Int. J. Chem. Kinet.* **1969**, *1*, 487–492.
[28] Olefin strain is defined as the difference in total strain energy between a cyclic olefin and its hydrogenated counterpart, both in their most stable conformation: W. F. Maier, P. von R. Schleyer, *J. Am. Chem. Soc.* **1981**, *103*, 1891–1900; *exo--exo* hydrogenation of HMDB yields an olefin strain of 4.2 kcal mol$^{-1}$.
[29] M. J. M. Vlaar, A. W. Ehlers, F. J. J. de Kanter, M. Schakel, A. L. Spek, K. Lammertsma, *Angew. Chem.* **2000**, *112*, 3071–3074; *Angew. Chem. Int. Ed.* **2000**, *39*, 2943–2945.
[30] a) A. Marinetti, F. Mathey, *Organometallics* **1984**, *3*, 456–461; b) A. Marinetti, F. Mathey, J. Fischer, A. Mitschler, *J. Am. Chem. Soc.* **1982**, *104*, 4484–4485; c) A. Marinetti, F. Mathey, *Organometallics* **1982**, *1*, 1488–1492.
[31] a) A. Marinetti, C. Charrier, F. Mathey, J. Fischer, *Organometallics* **1985**, *4*, 2134–2138; b) N. H. T. Huy, Y. Inubushi, L. Ricard, F. Mathey, *Organometallics* **1997**, *16*, 2506–2508.
[32] K. Lammertsma, A. W. Ehlers, M. L. McKee, *J. Am. Chem. Soc.* **2003**, *125*, 14750–14759.
[33] The aromatization of HMDB (**9**) to hexamethylbenzene is thermally forbidden, and the half-life of **9** is more than 21 h at 120 °C: W. J. le Noble, K. R. Brower, C. Brower, S. Chang, *J. Am. Chem. Soc.* **1982**, *104*, 3150–3152. Thus, the phosphinidene precursor **16** can be used at 110 °C without a catalyst, which precludes diphosphene formation.
[34] a) J. Furukawa, N. Kawabata, J. Nishimura, *Tetrahedron* **1968**, *24*, 53–58; b) I. Arai, A. Mori, H. Yamamoto, *J. Am. Chem. Soc.* **1985**, *107*, 8254–8256.
[35] Conversion after 45 min; 47% starting material was still present. The modest stability of the $W(CO)_5$ moiety in DCM precludes extensive reaction times.
[36] H. E. Gottlieb, V. Kotlyar, A. Nudelman, *J. Org. Chem.* **1997**, *62*, 7512–7515.
[37] A. J. M. Duisenberg, L. M. J. Kroon-Batenburg, A. M. M. Schreurs, *J. Appl. Crystallogr.* **2003**, *36*, 220–229.
[38] G. M. Sheldrick, SADABS: Area-Detector Absorption Correction, v2.10, Universität Göttingen, Göttingen (Germany), **1999**.
[39] P. T. Beurskens, G. Admiraal, G. Beurskens, W. P. Bosman, S. Garcia-Granda, R. O. Gould, J. M. M. Smits, C. Smykalla, The DIRDIF99 program system, Technical Report of the Crystallography Laboratory, University of Nijmegen, Nijmegen (The Netherlands), **1999**.
[40] G. M. Sheldrick, SHELXL-97: Program for crystal structure refinement, Universität Göttingen, Göttingen (Germany), **1997**.
[41] A. L. Spek, *J. Appl. Crystallogr.* **2003**, *36*, 7–13.

Received: June 22, 2007
Published online: November 21, 2007

  